

Triaxiality softness and shape coexistence in Mo and Ru isotopesH. Abusara,^{1,*} Shakeb Ahmad,^{2,†} and S. Othman¹¹*Department of Physics, BirZeit University, Ramallah, Palestine*²*Physics Section, Women's College, Aligarh Muslim University, Aligarh - 202002, India*

(Received 10 February 2017; published 4 May 2017)

A systematic search of triaxial ground state and shape coexistence in Ru and Mo isotopes is done using the relativistic-Hartree-Bogoliubov formalism using density-dependent zero and finite range NN interactions, and with separable pairing. Shape coexistence and triaxiality softness manifest themselves in a clear manner in Mo isotopes and only triaxiality softness is very clear in all of the Ru isotopes. Both point-coupling and meson-exchange models give similar results with few exceptions. A very good agreement is found with the available experimental data and with the macro-microscopic finite range droplet model. The findings are also in good agreement with the self-consistent Hartree-Fock-Bogoliubov calculations based on the interaction Gogny-D1S force.

DOI: [10.1103/PhysRevC.95.054302](https://doi.org/10.1103/PhysRevC.95.054302)**I. INTRODUCTION**

Several attempts have been made in the past decades to explain the shape coexistence in the atomic nuclei [1,2]. Many nuclear phenomena that are linked to the existence of triaxiality, such as wobbling motion in the rare-earth region [3] and chiral structures in the lanthanide region [4], are considered as evidences of shape coexistence. A nucleus may take different shapes varying from spherical to quadrupole, octupole, and higher order multipole deformations. These shapes are a consequence of the sensitive interplay between collective degrees of freedom and single particle energies. This interplay will lead to phase transition along an isotopic and isotonic chain [5]. A systematic review of the existing experimental data and the theoretical models of nuclei in different regions of the nuclear chart such as in the $Z \approx 40$ and $N \approx 60$ has been done in Ref. [1]. The mass region $A \approx 100$, represents a fertile ground for the search and study of shape coexistence [6–9], since it has been characterized by a shape instability, and thus shape coexistence is highly predicted in this region. Shape evolution for several isotopic chains in this region has been studied through the self-consistent mean-field (SCMF) approximation based on the Gogny-D1M energy density functional (EDF) [8,9], the potential energy surfaces (PES) using Skyrme HF+BCS [10], and relativistic mean field (RMF) with BCS pairing [11].

The isotopic chain of Mo, was recently under extensive study both experimentally and theoretically [8,12–18]. The different models used are the Coulomb excitation [12–14], microscopic Bohr collective model [15], and self-consistent Hartree-Fock-Bogoliubov (HFB) calculations based on the interaction Gogny D1S [16]. However, very recently Nomura *et al.* [8,9] has done a detail theoretical study based on Gogny-like interactions. In particular, the structural evolution of even-even Ru, Mo, Zr, Sr nuclei [8], and Ge, Se nuclei [9] have been studied within the SCMF approximation based on

the Gogny-D1M energy density functional. This calculation has fully explored the triaxial degrees of freedom and the shape coexistence in these nuclei. The spectroscopic properties have also been done for these nuclei with the help of a fermion-to-boson mapping procedure. This is very important as to clarify to which extent both triaxiality and shape coexistence are reflected in the spectroscopic properties of these nuclei. A $\gamma\gamma$ angular correlation experiment has been performed for selected Mo isotopes [17,18]. In this experiment, spin assignments, multipole matrix ratios, and lifetimes showed evidences for the shape coexistence in ^{96,98}Mo. The experimental findings are theoretically supported by the potential energy surface (PES) studies using the Skyrme density functional with SLy6 functional.

In the present analysis, we have done a systematic calculation in the search of triaxial ground state properties and shape coexistence for ^{92–108}Mo and ^{96–112}Ru isotopes. The systematic constrained triaxial calculation is done in the self-consistent mean field model—the relativistic-Hartree-Bogoliubov (RHB) with density-dependent zero and finite range NN interactions. The model parameters used are the density-dependent DD-ME2 [19] and DD-PC1 [20]. Pairing correlations are considered in the separable pairing model [21]. A systematic comparison is made with calculated values and experimental data [22–25], macro-microscopic finite range droplet model (FRDM) [26] as well as with the self-consistent HFB calculations based on the interaction Gogny-D1S force [27].

This paper is organized as follows. In Sec. II a general overview of the RHB formalism is presented. The numerical results of the calculations are discussed and compared with the results from others in Sec. III. Summary and conclusions are in Sec. IV.

II. THEORETICAL FRAMEWORK

In covariant density functional theory (CDFT) different models are used to describe the nucleus [19,20,28–30]. In this article we will use two types of these models, mainly: the density-dependent meson-exchange model and a density-dependent point-coupling model. In the first model the range

*Corresponding author: habusara@birzeit.edu†physics.sh@gmail.com

of the interaction is finite and related to the mass of the meson, while in the second model the mesons are absent and thus uses a zero range interaction. Each of these models is represented here by their corresponding parameter sets as DD-ME2 [19] and DD-PC1 [20]. They provide a very successful and an excellent description of different ground states and excited states over the entire periodic table [19,31–34]. The details of each model are discussed below.

A. Lagrangian density for the meson-exchange model

In the meson-exchange models [19], the nucleus is described as a system of point-like nucleon, Dirac spinors, interacting via the exchange of mesons with finite masses leading to the interactions of finite range. The starting point of CDFT is a standard Lagrangian density [35]

$$\begin{aligned} \mathcal{L} = & \bar{\psi}(\gamma(i\partial - g_\omega\omega - g_\rho\vec{\rho}\vec{\tau} - eA) - m - g_\sigma\sigma)\psi \\ & + \frac{1}{2}(\partial\sigma)^2 - \frac{1}{2}m_\sigma^2\sigma^2 - \frac{1}{4}\Omega_{\mu\nu}\Omega^{\mu\nu} + \frac{1}{2}m_\omega^2\omega^2 \\ & - \frac{1}{4}\vec{R}_{\mu\nu}\vec{R}^{\mu\nu} + \frac{1}{2}m_\rho^2\vec{\rho}^2 - \frac{1}{4}F_{\mu\nu}F^{\mu\nu} \end{aligned} \quad (1)$$

which contains nucleons described by the Dirac spinors ψ with the mass m and several effective mesons characterized by the quantum numbers of spin, parity, and isospin. They create effective fields in a Dirac equation, which corresponds to the Kohn-Sham equation [36] in the nonrelativistic case.

The Lagrangian (1) contains as parameters the meson masses m_σ , m_ω , and m_ρ and the coupling constants g_σ , g_ω , and g_ρ . e is the charge of the protons and it vanishes for neutrons. The density-dependent meson-nucleon coupling model has an explicit density dependence for the meson-nucleon vertices. The coupling constant dependence is defined as

$$g_i(\rho) = g_i(\rho_{\text{sat}})f_i(x), \quad (2)$$

i can be any of the three mesons σ , ω , and ρ where the density dependence is given by

$$f_i(x) = a_i \frac{1 + b_i(x + d_i)^2}{1 + c_i(x + d_i)^2} \quad (3)$$

for σ and ω and by

$$f_\rho(x) = \exp(-a_\rho(x - 1)) \quad (4)$$

for the ρ meson. x is defined as the ratio between the baryonic density ρ at a specific location and the baryonic density at saturation ρ_{sat} in symmetric nuclear matter. The eight parameters in Eq. (3) are not independent, but constrained as follows: $f_i(1) = 1$, $f_\sigma''(1) = f_\omega''(1)$, and $f_i'(0) = 0$. These constraints reduce the number of independent parameters for density dependence to three. This model is represented in the present investigations by the parameter set DD-ME2 [19].

B. Lagrangian density for the point-coupling model

In complete analogy to the meson-exchange phenomenology, the point-coupling model represents an alternative formulation of the self-consistent relativistic mean-field framework [20,37–40]. The effective Lagrangian for the density-dependent point-coupling model [20,41] that includes the isoscalar-scalar, isoscalar-vector, and isovector-vector four-

fermion interactions is given by

$$\begin{aligned} \mathcal{L} = & \bar{\psi}(i\gamma \cdot \partial - m)\psi \\ & - \frac{1}{2}\alpha_S(\hat{\rho})(\bar{\psi}\psi)(\bar{\psi}\psi) - \frac{1}{2}\alpha_V(\hat{\rho})(\bar{\psi}\gamma^\mu\psi)(\bar{\psi}\gamma_\mu\psi) \\ & - \frac{1}{2}\alpha_T V(\hat{\rho})(\bar{\psi}\vec{\tau}\gamma^\mu\psi)(\bar{\psi}\vec{\tau}\gamma_\mu\psi) \\ & - \frac{1}{2}\delta_S(\partial_\nu\bar{\psi})(\partial^\nu\bar{\psi}) - e\bar{\psi}\gamma \cdot A \frac{(1 - \tau_3)}{2}\psi. \end{aligned} \quad (5)$$

It contains the free-nucleon Lagrangian, the point-coupling interaction terms, and, in addition to these two, the model includes the coupling of the proton to the electromagnetic field. The derivative terms in Eq. (5) accounts for the leading effects of finite-range interactions that are crucial for a quantitative description of the nuclear properties. The functional form of the point-couplings chosen is

$$\alpha_i(\rho) = a_i + (b_i + c_i x)e^{-d_i x}, \quad (i = S, V, TV), \quad (6)$$

where $x = \rho/\rho_{\text{sat}}$, and ρ_{sat} denotes the nucleon density at saturation in symmetric nuclear matter. In the present work, we have used the recently developed density-dependent point-coupling interaction DD-PC1 [20]. In the current investigation, the triaxial RHB with separable pairing model is used (for more details see Refs. [21,42]).

The constrained calculations are performed by imposing constraints on both axial and triaxial mass quadrupole moments. The potential energy surface (PES) study as a function of the quadrupole deformation parameter is performed by the method of quadratic constrained [43]. The method of quadratic constraints uses an unrestricted variation of the function

$$\langle \hat{H} \rangle + \sum_{\mu=0,2} C_{2\mu} (\langle \hat{Q}_{2\mu} \rangle - q_{2\mu})^2, \quad (7)$$

where $\langle \hat{H} \rangle$ is the total energy, $\langle \hat{Q}_{2\mu} \rangle$ denotes the expectation values of mass quadrupole operators,

$$\hat{Q}_{20} = 2z^2 - x^2 - y^2 \quad \text{and} \quad \hat{Q}_{22} = x^2 - y^2, \quad (8)$$

$q_{2\mu}$ is the constrained value of the multipole moment, and $C_{2\mu}$ is the corresponding stiffness constant [43]. Moreover, the quadratic constraint adds an extra force term $\sum_{\mu=0,2} \lambda_\mu \hat{Q}_{2\mu}$ to the system, where $\lambda_\mu = 2C_{2\mu} (\langle \hat{Q}_{2\mu} \rangle - q_{2\mu})^2$ for a self-consistent solution. This term is necessary to force the system to a point in deformation space different from a stationary point. The augmented Lagrangian method [44] has also been implemented in order to resolve the problem of convergence of the self-consistent procedure which diverges while increasing the value of stiffness constant $C_{2\mu}$ used in the procedure.

III. RESULTS AND DISCUSSION

Both Mo and Ru lie in the region where deformation is mainly due to the filling of the $N = 50$ shell gap. Thus sudden changes in nuclear shape [1], shape coexistence, and triaxial ground state [45–50] are expected. Systematic constrained triaxial calculations mapping the quadrupole deformation

TABLE I. Location of the ground state indicated by (β^0, γ^0) for Ru isotopes using DD-ME2 and DD-PC1 parametrizations.

Nucleus	DD-ME2	DD-PC1
^{96}Ru	(0.15, 10°)	(0.15, 5°)
^{98}Ru	(0.22, 20°)	(0.18, 5°)
^{100}Ru	(0.25, 05°)	(0.23, 5°)
^{102}Ru	(0.25, 15°)	(0.25, 17°)
^{104}Ru	(0.25, 22°), (0.4, 0°)	(0.27, 22°)
^{106}Ru	(0.25, 25°)	(0.27, 22°)
^{108}Ru	(0.25, 40°)	(0.25, 40°)
^{110}Ru	(0.23, 55°)	(0.23, 55°)
^{112}Ru	(0.24, 55°)	(0.24, 55°)

space defined by β_2 and γ have been performed for $^{92-108}\text{Mo}$ and $^{96-112}\text{Ru}$ isotopes, using both DD-ME2 and DD-PC1 parametrizations. For each nuclei two contour plots have been made one each parametrization to investigate the location of a triaxial ground state, and the possibility of shape coexistence. The location of the ground state in the β - γ deformation space is indicated by the point (β^0, γ^0) .

The location of the ground state is shown in Table I for Ru isotopes and in Table II for Mo isotopes and is extracted from Figs. 1, 2, 3, and 4. In Figs. 1 and 2, we show the contour plots for Ru isotopes using DD-ME2 and DD-PC1 parameter sets, respectively. As can be seen from Fig. 1 the ground state for the lightest considered Ru ($N = 52$) isotopes is weakly deformed and soft in the γ direction. As the number of neutrons increases the value of β_2 deformation in the ground state increases and the shape starts to deviate from the spherical shape and starts to be axially deformed (oblate). But the softness in the γ direction becomes stronger. As we reach $N = 60$, we notice that the ground state becomes triaxial and still soft in the γ direction. The potential energy surfaces indicate the existence of an axial minimum in addition to the triaxial minimum. The axial minimum is located near $\beta_2 = 0.4$ and $\gamma = 0$. The difference in energy between these two minimums is around 0.3 MeV. This a clear suggestion of shape coexistence in ^{104}Ru . However, this minimum disappears for $N = 62$ and does not show up in the DD-PC1 results shown in Fig. 2. Thus we tend to think that shape coexistence does not exist in this nuclei.

 TABLE II. Location of the ground state indicated by (β^0, γ^0) for Mo isotopes using DD-ME2 and DD-PC1 parametrizations.

Nucleus	DD-ME2	DD-PC1
^{92}Mo	(0.0, 0°)	(0.0, 0°)
^{94}Mo	(0.15, 10°)	(0.05, 35°)
^{96}Mo	(0.23, 25°), (0.20, 0°)	(0.22, 22°)
^{98}Mo	(0.25, 10°)	(0.22, 32°), (0.23, 10°)
^{100}Mo	(0.25, 20°), (0.22, 60°)	(0.25, 20°)
^{102}Mo	(0.33, 20°), (0.40, 0°)	(0.33, 20°)
^{104}Mo	(0.37, 17°), (0.22, 55°)	(0.38, 17°), (0.23, 55°)
^{106}Mo	(0.39, 17°), (0.22, 55°)	(0.36, 17°), (0.23, 55°)
^{108}Mo	(0.37, 20°), (0.24, 55°)	(0.37, 20°), (0.24, 55°)

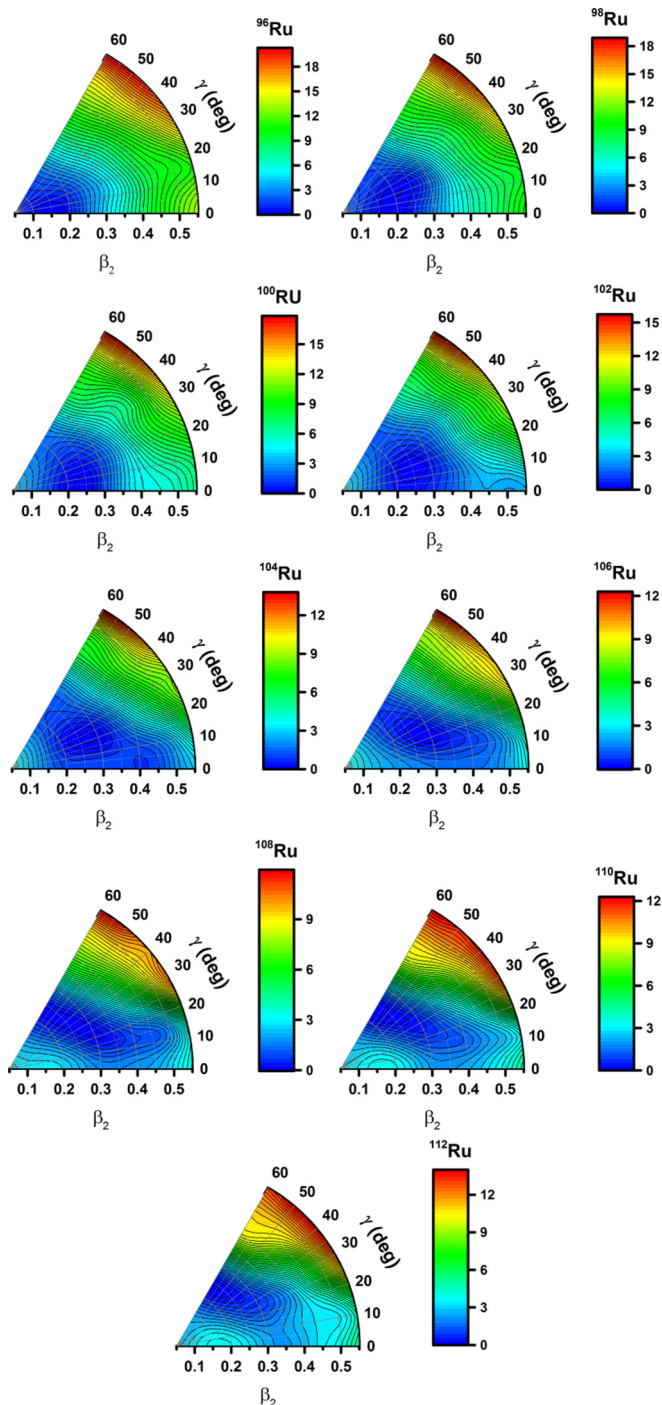


FIG. 1. Potential energy surfaces of the Ru isotopes from neutron number $N = 52$ to 68 in the (β, γ) plane, obtained from a triaxial RHB calculations with the DD-ME2 parameter set. The color scale shown at the right has the unit of MeV, and scaled such that the ground state has a zero MeV energy.

Further, as the number of neutrons increases to $N = 64$ and beyond, the ground state minimum moves from the triaxial shape into an axial oblate shape. These results are in full agreement with the results shown in Fig. 1 of Ref. [8] using the IBM based on Gogny-D1M energy density functional theory. However, Fig. 32 in [1] shows static and dynamic

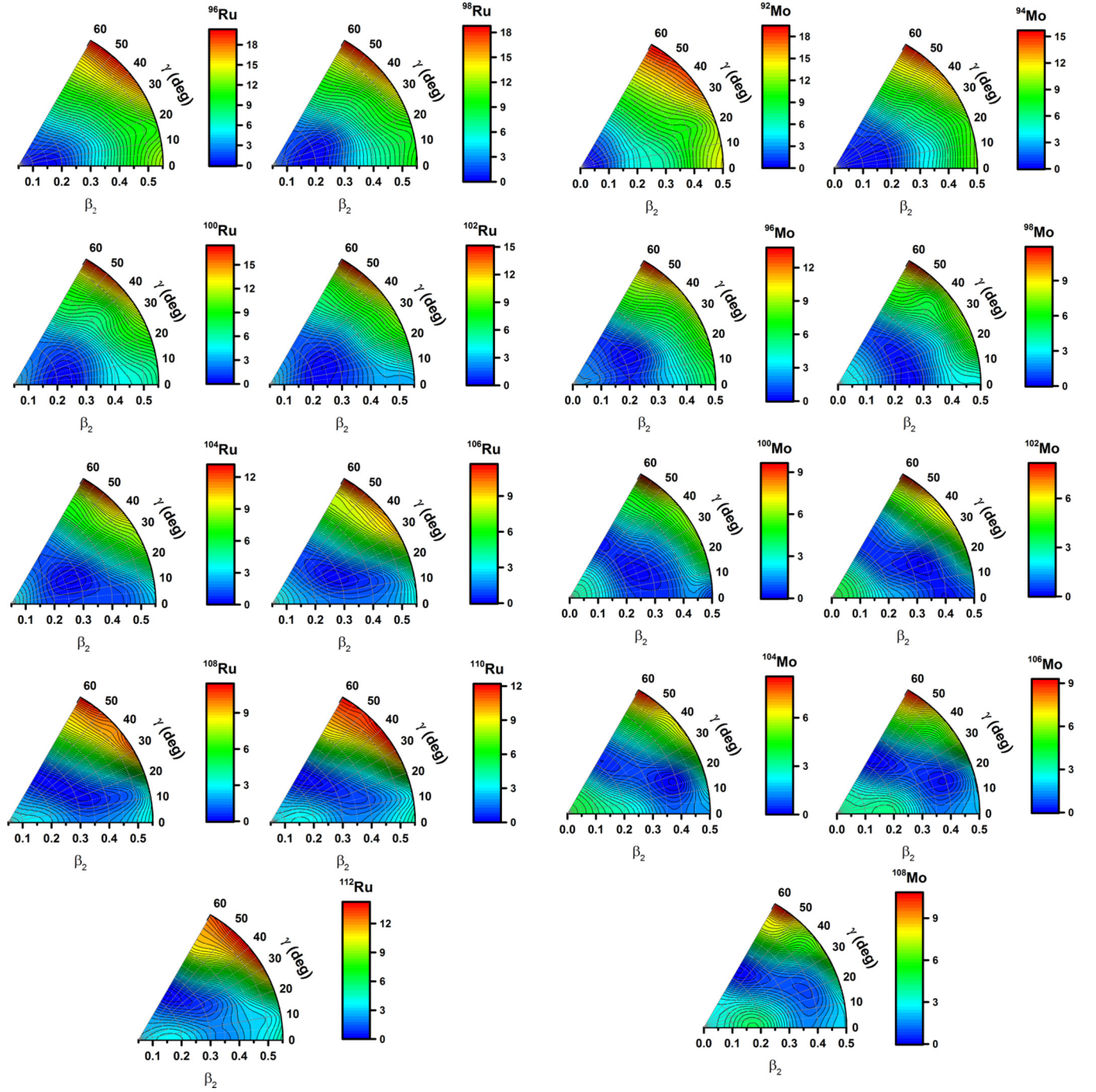


FIG. 2. The same as in Fig. 1, but with different parameter set DD-PC1.

quadrupole moment data, which suggests the presence of shape coexistence in ^{104}Ru .

The existence of two shapes is better seen in the case of Mo isotopes than in the case of Ru isotopes. In $^{92,94}\text{Mo}$, the ground state is nearly spherical with some degree of γ softness. However, ^{94}Mo is more deformed, near prolate, than ^{92}Mo . Triaxial shape ground state starts to manifest itself in ^{96}Mo , and as the number of neutrons increases, γ softness and shape coexistence become clearer. In Table II we list the ground state

FIG. 3. Potential energy surfaces of the Mo isotopes from neutron number $N = 50$ to 66 in the (β, γ) plane, obtained from a triaxial RHB calculations with the DD-ME2 parameter set. The color scale shown at the right has units of MeV, and scaled such that the ground state has a 0 MeV energy.

deformation of all the Mo isotopes. In DD-ME2 calculations the potential energy surfaces of the following nuclei are found to possess two ground state minimum, $^{96,100,102,104,106,108}\text{Mo}$, while $^{92,94,98}\text{Mo}$ have only one.

$^{96,102}\text{Mo}$ have a triaxial and prolate axial minimum, and the difference in energy between the two minima is around 0.3 and 0.17 MeV, respectively. On the other hand, $^{100,104,106,108}\text{Mo}$

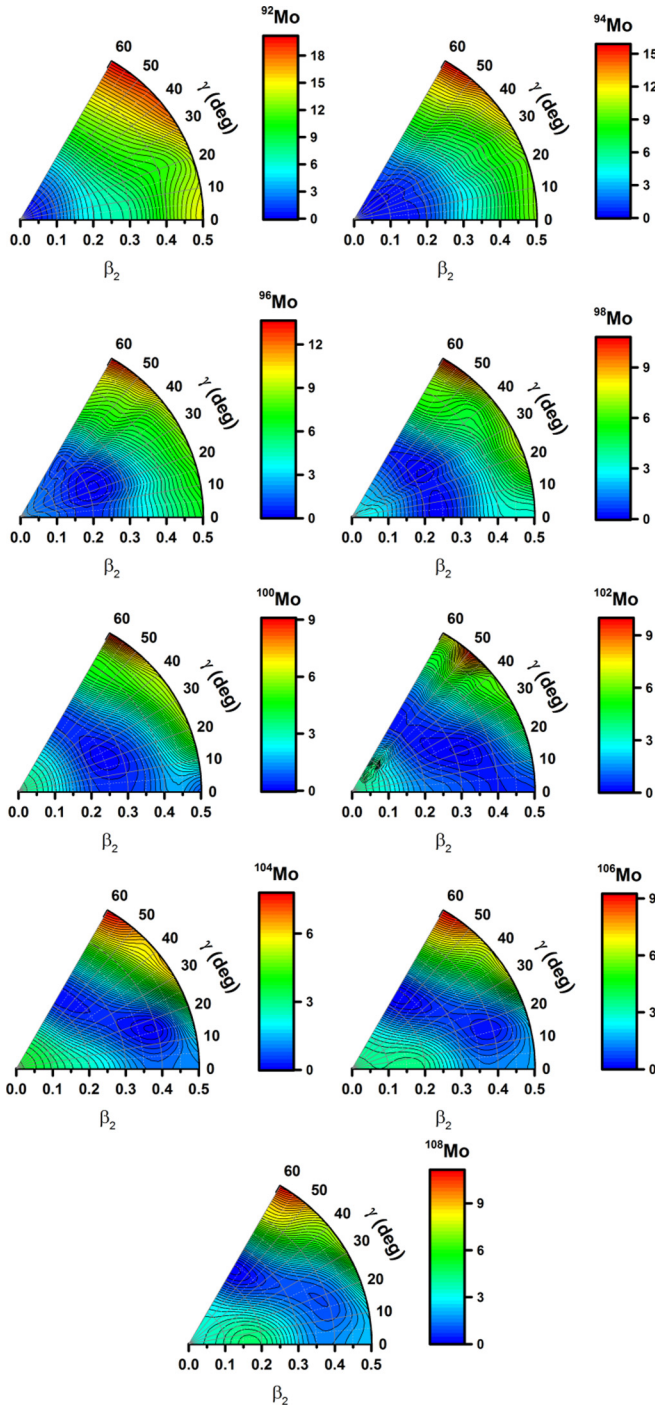


FIG. 4. The same as in Fig. 3, but with different a parameter set DD-PC1.

have a triaxial and oblate ground state with an energy difference between the two minima is 0.2 MeV for ^{100}Mo , 0.17 MeV for ^{104}Mo , zero for ^{106}Mo , and up to 0.9 MeV for ^{108}Mo .

The DD-PC1 calculations slightly vary from the DD-ME2, it suggests that only $^{98,104,106,108}\text{Mo}$ displays multiple minima. ^{98}Mo has two triaxial ground state minima, while $^{104,106}\text{Mo}$ has triaxial and axial (oblate) ground states. The difference

in binding energy between the two minima is 0.18 MeV for ^{98}Mo , 0.3 MeV for ^{104}Mo , 0.2 MeV in ^{106}Mo , and 0.9 MeV for ^{108}Mo .

We can notice that with an increase of the number of neutrons the ground state minimum becomes near oblate and the difference in energy between the two minimum increases, thus one would expect there is no shape coexistence beyond ^{108}Mo . This indeed is in agreement with the results of Ref. [8], with the results in Fig. 6 of Ref. [16] and the results from Ref. [11].

The main difference between the results of DD-ME2 and DD-PC1 is that γ softness covers a wider range of values of γ deformation in the case of the DD-PC1 than what obtained with DD-ME2, thus eliminating the possibility of the formation of a new minimum.

The transition of the ground state along the isotopic chains of Mo and Ru is smooth. This is well seen in Figs. 1, 2, 3, and 4, where at the beginning of the isotopic chain the location of the ground state minimum moves from near prolate shape at the beginning of the chain to near the oblate shape at its other end. This is due to the development of a maximum or what looks like a hill pushing the ground state minimum away from the spherical shape into an a near prolate minimum as can be seen for Ru isotopes. For example, in Fig. 1 the ground state for ^{96}Ru is near spherical, and the uprising hill is pushing it to the right to become axial (prolate). The hill size is increasing and starts to push the ground state to be triaxial and away from the prolate or oblate shapes as seen in ^{104}Ru . Finally pushing it to be near oblate in starting from ^{108}Ru . Thus, one can see that the shape transition is smooth through the wide range of triaxiality, and there are no sudden changes in the nuclear shape. This is in full agreement with the results obtained with HFB based on Gogny-D1S interaction [27], Gogny-D1M [8], and relativistic mean field [11].

One can relate this smooth transition of the ground state along the isotopic chains with the evolution of several ground state nuclear properties along an isotopic chain. For that we study the evolution of binding energy (BE), proton radii (R_p) and neutron radii (R_n), two neutron separation energies (S_{2n}), and root mean square charge radii (R_c) with $\delta\langle r_c^2 \rangle^{50,N} = \langle r_c^2 \rangle^N - \langle r_c^2 \rangle^{50}$, for both Ru and Mo isotopic chains and the results are shown in Figs. 5, 6, 7, 8, 9, and 10. The plotted values are taken at the ground state defined in Tables I and II.

Figures 5 and 6 show the results of the total BE and binding energy per nucleon (BE/A) for Mo and Ru isotopic chains, calculated using the RHB model with density dependent force parameters DD-ME2 and DD-PC1. The results vary smoothly with an increase of the number of neutrons. The comparison is shown with the available experimental data [22] and with the predictions made by the macro-microscopic finite range droplet model (FRDM) [26]. It is seen that our results are in good agreement with each other and with the experimental data. However, the results with DD-ME2, differ slightly with a constant factor throughout the region of study.

In Fig. 7, we show two neutron separation energies (S_{2n}), and compared with the available experimental data [22–25] and FRDM [26]. It can be seen that our calculations reproduce well the experimental separation energies. The results for the neutron (R_n) and proton radii (R_p) and the root mean square

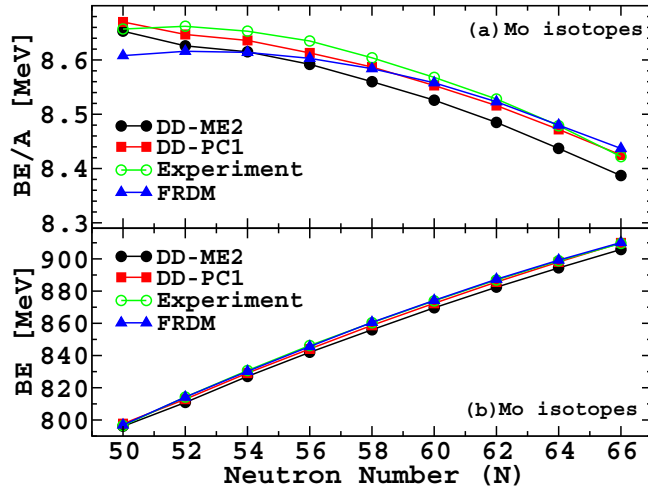


FIG. 5. Binding energy per nucleon (a) and the total binding energy (b) of the Mo isotopes using both DD-ME2 and DD-PC1 as a function of neutron number. Comparison with FRDM [26] results and experimental data [22] are shown.

charge radii (R_c) are shown in Figs. 8 and 9, respectively. Results obtained for $\delta(r_c^2)^{50,N}$ are also shown in Fig. 10. Our results for R_n , R_p , and R_c and their indication of the smooth transition of the nuclear shape are consistent with the results obtained in Fig. 3 in Ref. [16]. There is a good agreement with the experimental data [16,23–25] available in case of rms charge radii. Overall results for the ground state bulk properties calculated are also found to be in agreement with the self-consistent HFB calculations based on the interaction Gogny-D1s force [27].

We notice all of these quantities are, in general, varying smoothly with the neutron numbers, which confirm our

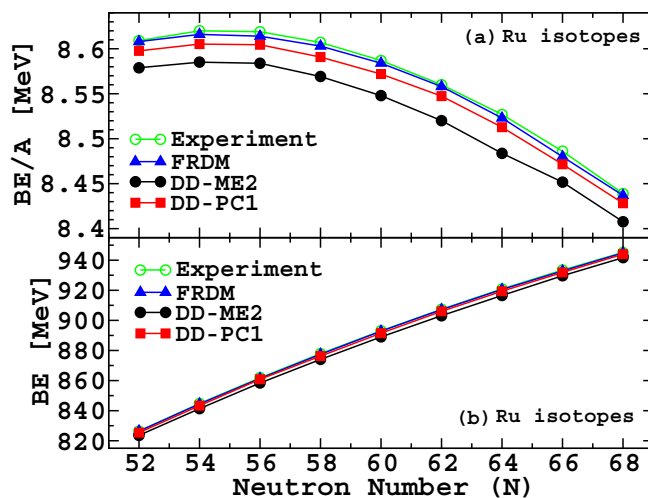


FIG. 6. Binding energy per nucleon (a) and the total binding energy (b) of the Ru isotopes using both DD-ME2 and DD-PC1 as a function of neutron number. Comparison with FRDM [26] results and experimental data [22] are shown.

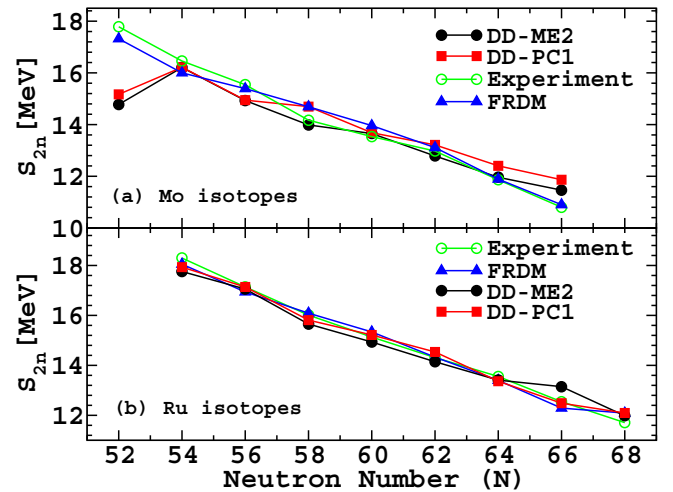


FIG. 7. Two neutron separations energies of Mo and Ru isotopes using both DD-ME2 and DD-PC1 as a function of neutron number. Comparison with FRDM [26] results and experimental data [22–25] are shown.

observation of a smooth transition in the ground state among the nuclei under consideration.

A systematic investigation of the ground state properties of these chains has been done in [51]. However, it is not clear whether they include triaxial degree of freedom in their calculations, in Fig. 8 they show the quadrupole deformation as a function of the neutron number, but there is no indication of the value of γ . However, since these chains show sign of triaxiality softness in the ground state, we can notice that our results shown in Tables I and II are consistent with the results of Fig. 8 in [51].

Our results are independent of the choice of the model used in covariant density functional theory and the parameter set. As we mentioned in the beginning of Sec. II, we have used two different models represented by two sets, DD-ME2 and DD-PC1. The obtained results from both of these models

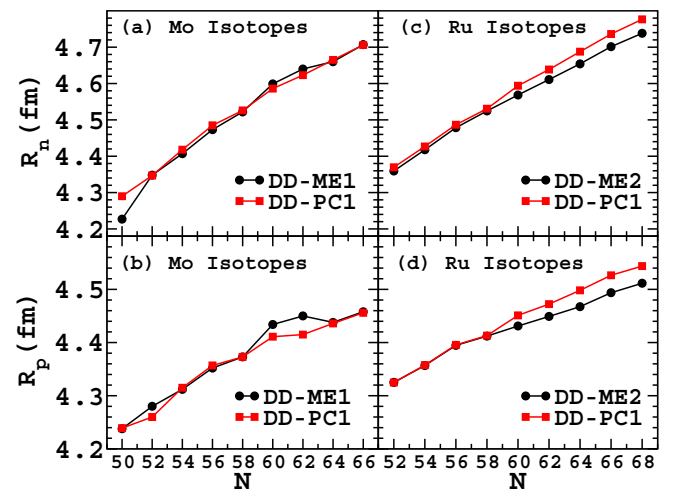


FIG. 8. Neutron and proton radii of Mo and Ru isotopes using both DD-ME2 and DD-PC1 as a function of neutron number.

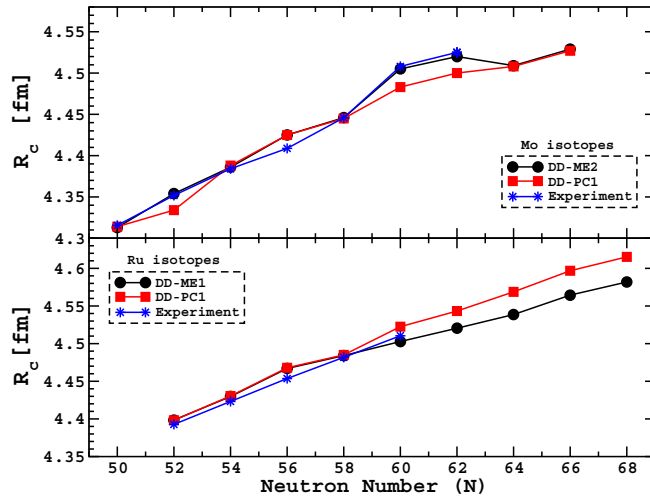


FIG. 9. Charge radius for Mo and Ru isotopes using both DD-ME2 and DD-PC1 as a function of neutron number, compared to experimental data from Ref. [25].

is consistent with each other with very limited variations. In Ref. [11] the authors use point coupling model and resort to the parameter set PC-K1, we used DD-PC1, and they show potential energy surfaces for the Mo isotopes in Fig. 5. The result is in good agreement with ours, mainly in the predication of shape coexistence, the smooth transition of the ground state and the smooth evolution of the charge radius with the neutron number.

IV. CONCLUSION

We have used the relativistic-Hartree-Bogoliubov (RHB) formalism with separable pairing to perform a systematic calculation along two isotopic chains, Ru and Mo, for the search of triaxial ground state and shape coexistence. The results of our investigation can be summarized as follows:

- (i) Shape coexistence does not show up in any of the Ru isotopes except in ^{104}Ru using DD-ME2 parametrization. But triaxiality softness is clear in all of these isotopes.

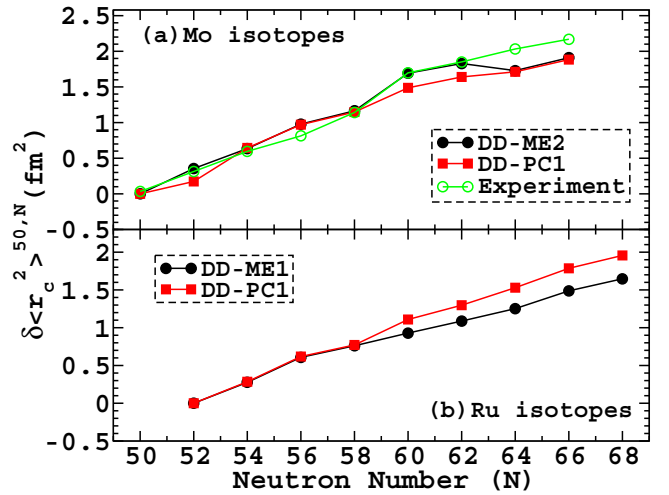


FIG. 10. $\delta \langle r_c^2 \rangle_{50,N}$ for Mo and Ru isotopes using both DD-ME2 and DD-PC1 as a function of neutron number, compared to experimental data from Refs. [23–25].

- (ii) Shape coexistence and triaxiality softness manifest themselves in a clear manner in Mo isotopes.
- (iii) At the beginning of each isotopic chain, the ground state has a near prolate shape, but as the number of neutrons increases the shape smoothly move into triaxiality and then into the near oblate shape toward the end of the chain.
- (iv) The results we obtained is independent of the choice of model and parameter set as it agrees with the results obtained in [11].
- (v) A comparison of our results with those in Refs. [8,16,27,51] shows very good agreement with the majority of the calculations.
- (vi) The results of the calculations for the ground state bulk properties are in good agreement with the available experimental data and FRDM. It also reflects the smooth transition of the ground state and the softness in the γ direction.

[1] J. L. Wood, K. Heyde, W. Nazarewicz, M. Huyse, and P. van Duppen, *Phys. Rep.* **215**, 101 (1992).
 [2] K. Heyde and J. L. Wood, *Rev. Mod. Phys.* **83**, 1467 (2011).
 [3] D. R. Jensen *et al.*, *Phys. Rev. Lett.* **89**, 142503 (2002).
 [4] S. Frauendorf, *Rev. Mod. Phys.* **73**, 463 (2001).
 [5] P. Cejnar, J. Jolie, and R. F. Casten, *Rev. Mod. Phys.* **82**, 2155 (2010).
 [6] V. Werner *et al.*, *Phys. Lett. B* **550**, 140 (2002).
 [7] G. S. Simpson, J. A. Pinston, D. Balabanski, J. Genevey, G. Georgiev, J. Jolie, D. S. Judson, R. Orlandi, A. Scherillo, I. Tsekhanovich, W. Urban, and N. Warr, *Phys. Rev. C* **74**, 064308 (2006).
 [8] K. Nomura, R. Rodríguez-Guzmán, and L. M. Robledo, *Phys. Rev. C* **94**, 044314 (2016).

[9] K. Nomura, R. Rodríguez-Guzmán, and L. M. Robledo, [arXiv:1702.04879v1](https://arxiv.org/abs/1702.04879v1) [nucl-th].
 [10] P. Bonche *et al.*, *Nucl. Phys. A* **443**, 39 (1985).
 [11] J. Xiang, Z. P. Li, Z. X. Li, J. M. Yao, and J. Meng, *Nucl. Phys. A* **873**, 1 (2012).
 [12] M. Zielinska *et al.*, *Acta Phys. Pol. B* **36**, 1289 (2005).
 [13] K. Wrzosek-Lipska *et al.*, *Int. J. Mod. Phys. E* **20**, 443 (2011).
 [14] K. Wrzosek *et al.*, *Int. J. Mod. Phys. E* **15**, 374 (2006).
 [15] L. Prochniak, *Int. J. Mod. Phys. E* **19**, 705 (2010).
 [16] R. Rodríguez-Guzmán, P. Sarrigurena, L. M. Robledo, and S. Perez-Martin, *Phys. Lett. B* **691**, 202 (2010).
 [17] T. Thomas, K. Nomura, V. Werner, T. Ahn, N. Cooper, H. Duckwitz, M. Hinton, G. Ilie, J. Jolie, P. Petkov, and D. Radeck, *Phys. Rev. C* **88**, 044305 (2013).

- [18] T. Thomasa, V. Werner, J. Jolie, K. Nomura, T. Ahn, N. Cooper, H. Duckwitz, A. Fitzler, C. Fransena, A. Gadea, M. Hinton, G. Ilie, K. Jessena, A. Linnemanna, P. Petkova, N. Pietrallac, and D. Radecka, *Nucl. Phys. A* **947**, 203 (2016).
- [19] G. A. Lalazissis, T. Nikšić, D. Vretenar, and P. Ring, *Phys. Rev. C* **71**, 024312 (2005).
- [20] T. Nikšić, D. Vretenar, and P. Ring, *Phys. Rev. C* **78**, 034318 (2008).
- [21] T. Nikšić, N. Paar, D. Vretenar, and P. Ring, *Comp. Phys. Comm.* **185**, 1808 (2014).
- [22] M. Wang, G. Audi, A. H. Wapstra *et al.*, *Chin. Phys. C* **36**, 1603 (2012).
- [23] F. C. Charlwood *et al.*, *Phys. Lett. B* **674**, 23 (2009).
- [24] U. Hager *et al.*, *Phys. Rev. Lett.* **96**, 042504 (2006).
- [25] I. Angeli, *At. Data Nucl. Data Table* **87**, 185 (2004).
- [26] P. Möller, J. R. Nix, and K.-L. Kratz, *At. Data Nucl. Data Tables* **66**, 131 (1997).
- [27] www-phynu.cea.fr/science_en_ligne/carte_potentiels_microscopiques/carte_potentiel_nucleaire_eng.htm.
- [28] T. Nikšić, D. Vretenar, P. Finelli, and P. Ring, *Phys. Rev. C* **66**, 024306 (2002).
- [29] X. Roca-Maza, X. Viñas, M. Centelles, P. Ring, and P. Schuck, *Phys. Rev. C* **84**, 054309 (2011).
- [30] N. Paar, D. Vretenar, E. Khan, and G. Coló, *Rep. Prog. Phys.* **70**, 691 (2007).
- [31] A. V. Afanasjev and H. Abusara, *Phys. Rev. C* **81**, 014309 (2010).
- [32] D. Vretenar, A. V. Afanasjev, G. A. Lalazissis, and P. Ring, *Phys. Rep.* **409**, 101 (2005).
- [33] T. Nikšić, D. Vretenar, and P. Ring, *Prog. Part. Nucl. Phys.* **66**, 519 (2011).
- [34] H. Abusara, A. V. Afanasjev, and P. Ring, *Phys. Rev. C* **85**, 024314 (2012).
- [35] Y. K. Gambhir, P. Ring, and A. Thimet, *Ann. Phys. (NY)* **198**, 132 (1990).
- [36] W. Kohn and L. J. Sham, *Phys. Rev.* **137**, A1697 (1965).
- [37] P. Manakos and T. Mannel, *Z. Phys. A* **330**, 223 (1988).
- [38] J. J. Rusnak and R. J. Furnstahl, *Nucl. Phys. A* **627**, 495 (1997).
- [39] T. Bürvenich, D. G. Madland, J. A. Maruhn, and P. G. Reinhard, *Phys. Rev. C* **65**, 044308 (2002).
- [40] P. W. Zhao, Z. P. Li, J. M. Yao, and J. Meng, *Phys. Rev. C* **82**, 054319 (2010).
- [41] B. A. Nikolaus, T. Hoch, and D. G. Madland, *Phys. Rev. C* **46**, 1757 (1992).
- [42] W. Koepf and P. Ring, *Nucl. Phys. A* **493**, 61 (1989).
- [43] P. Ring and P. Schuck, *The Nuclear Many-Body Problem* (Springer-Verlag, Berlin, 1980).
- [44] A. Staszack, M. Stoitsov, A. Baran, and W. Nazarewicz, *Eur. Phys. J. A* **46**, 85 (2010).
- [45] *Nuclear Structure of the Zirconium Region*, edited by J. Eberth, R. A. Meyer, and K. Sistemich (Springer, Berlin, 1988).
- [46] J. Stachel, N. Karella, E. Grosse, H. Emling, H. Folger, R. Kulesa, and D. Schwalm, *Nucl. Phys. A* **383**, 429 (1982).
- [47] J. Srebrny, T. Czosnyka, and C. Droste, *Nucl. Phys. A* **766**, 25 (2006).
- [48] Y. Luo, S. Zhu, J. Hamilton, J. Rasmussen, A. Ramayya, C. Goodin, K. Li, J. Hwang, D. Almed, S. Frauendorf, V. Dimitrov, J. ye Zhang, X. Che, Z. Jang, I. Stefanescu, A. Gelberg, G. Ter-Akopian, A. Daniel, M. Stoyer, R. Donangelo, J. Cole, and N. Stone, *Phys. Lett. B* **691**, 285 (2010).
- [49] Wrzosek-Lipska, *Phys. Rev. C* **86**, 064305 (2012).
- [50] A. G. Smith, J. L. Durell, W. R. Phillips, W. Urban, P. Sarriguren, and I. Ahmad, *Phys. Rev. C* **86**, 014321 (2012).
- [51] Y. ElBassem and M. Oulne, *Nucl. Phys. A* **957**, 22 (2017).